SLAC-PUB-9643
March 2003

Performance of Large Area Silicon Strip Sensors for GLAST

S. Yoshida, H. Masuda, T. Ohsugi, Y. Fukazawa, K. Yamanaka, H.F.W. Sadrozinski, Senior *Member, IEEE*, T. Handa, A. Kavelaars, A. Brez, R. Bellazzini, L. Latronico, K. Yamamura, K. Yamamoto, K. Sato

***Abstract*--We report on the performance of silicon strip sensors for GLAST, produced by Hamamatsu Photonics, Japan. The size of the sensors is 89.5 mm× 89.5 mm and they were processed on 6 inch high resistivity wafers. By now, over 1,000 of ultimately 11,500 sensors have been produced and 622 have been investigated in detail. The average leakage current density is only 3.4 nA/cm^2 at 25 ^{o}C. Such a low leakage current density enables us to screen out a sensor having few strips with high leakage current by looking at the total sensor leakage current, instead of measuring individual strip currents. High breakdown voltage is also achieved. Of 10 sensors investigated for high voltage breakdown, all hold bias voltage up to 500 V without significant increase in the leakage current. The faulty strip rate is about 0.01 % of 240 k strips tested.**

I. Introduction

GLAST (Gamma-ray Large Area Space Telescope) is a satellite space mission, which will be launched by NASA in 2006. The main instrument on GLAST is the Large Area Telescope (LAT) [1], [2]. The GLAST LAT is a highly modular instrument composed of an 4×4 array of tracker (TKR) and calorimeter (CAL) towers, enclosed by an anti-coincidence shield (ACD). The GLAST LAT detects the gamma-ray using electron-positron conversion. The TKR measures the angle of electrons and positrons, and the CAL measures the energy of the gamma-ray.

Silicon strip sensors are used as tracking detectors in the TKR of GLAST LAT [3], [4]. The total number of sensors for GLAST LAT is about 10,000 and the total area of sensors is about 80 m^2. The use of silicon strip sensors is the big improvement over the previous successful EGRET experiment [5], which used spark chambers. Silicon strip sensors have high resolution and they are fast, resulting in negligible dead time. They also have no consumables so the lifetime of the sensors is longer than the 5 years of the GLAST mission. GLAST LAT is expected to have 100 times better source sensitivity than EGRET [6], [7].

The use of silicon strip sensors in space requires special attention to their performance, and to radiation damage as well, in addition to other space specific issues. The expected on-orbit total dose rate for the GLAST silicon sensors is about 200 rd per year during minimum solar activity. The total dose for the 5 year GLAST mission is thus estimated to be 1 krd, and the requirement is 5 krd when a 5x design margin is included [8]. There are also Single-Event Effects (SEE) to be considered due to single heavily ionizing ions. The GLAST requirement is to be SEE tolerant up to a LET > 8 MeV/(mg/cm^2). The results of our investigation of the SEE effects are reported in a companion paper [9]. In this paper we report on the radiation damage due to gamma-rays from ^{60}Co, in addition to the basic performance of the sensors.

II. Performance of the Sensors

The sensors for GLAST LAT are single-sided, p^+-strip in n-bulk with 40 MΩ bias resistors, AC-coupled and designed by Hiroshima University, manufactured by Hamamatsu Photonics (HPK). A sensor is diced from 6-inch silicon wafer to an outside dimension of 89.5 mm × 89.5 mm, and its sensitive area is 87.6 mm × 87.6 mm. The thickness of the sensor is 410 μm. The number of strips is 384 and the strip pitch is 228 μm. The widths of the p^+ implant strip and of the readout aluminum strip are 56 μm and 64 μm, respectively. The coupling dielectric between the p^+ strip and the aluminum strip has double layer structure. There is a 0.22 μm thick SiO_2 layer on the p^+ strip and a 0.1 μm thick Si_3N_4 layer underneath the aluminum strip. Each sensor has a guard-ring, which is left electrically floating at all times.

More than 1,000 sensors have been produced and 622 sensors have been measured in detail. We report their performance in the following. All of the measurements and irradiation were done at atmospheric pressure.

A. Full Depletion Voltage

The bias voltage dependence of the sensor bulk capacitance has been measured at 100 Hz for all sensors by HPK. Some

Manuscript received Nov 23, 2001. This work was supported by the Japan-US cooperative program in the field of high energy physics and Grant-in-Aid for Encouragement of Young Scientists.

S. Yoshida, H. Masuda, T. Ohsugi, Y. Fukazawa and K. Yamanaka are with Hiroshima University, Higashi-Hiroshima, 739-8526, Japan (e-mail: yoshidas@hiroshima-u.ac.jp).

H.F.W. Sadrozinski is with SCIPP, UCSC, Santa Cruz, CA 93106-9530 USA. T. Handa and A. Kavelaars are with SLAC, 2575 Sand Hill Road, CA 94025 USA. A. Brez , R. Bellazzini and L. Latronico are with INFN-Pisa and University of Pisa, 1-56010, Pisa, Italy.

Y. Yamamura, K. Yamamoto and K. Sato are with Hamamatsu Photonics, Hamamatsu , 435-8558, Japan.

Work supported in part by the Department of Energy contract DE-AC03-76SF00515.
Stanford Linear Accelerator Center, Stanford, University, Stanford, CA 94309

examples of C-V curves are shown in Fig. 1. To allow an easier determination of the full depletion voltage, at which the bulk capacitance saturates, the inverse square of the capacitance is plotted in Fig. 1. The saturation is clearly seen at about 60 V, and the full depletion voltage is defined as the voltage at which the slope in Fig. 1 becomes less than 8^{14} $(1/F^2)/V$. The distribution of the full depletion voltage for 622 sensors is shown in Fig. 2, extending from 40 V to 135 V, with only one sensor exceeding the specification of 120 V. Two lobes appear in the distribution of the full depletion voltage: one centered at 60 V and the other centered at 95 V. This difference can be explained by different resistivity values of the blank wafers bought at different points in time. The average value of full depletion voltage is 63 ± 13 V. This full depletion voltage is relatively low for 410 μm thick sensor and is due to the use of wafers with the high resistivity of 10 ± 2 kΩcm. At this high value, it is hard to control the resistivity, hence the rather large spread. The operation of sensors under the low bias voltage is very desirable for a space mission, where the power is limited and high voltages create a potential for arcing.

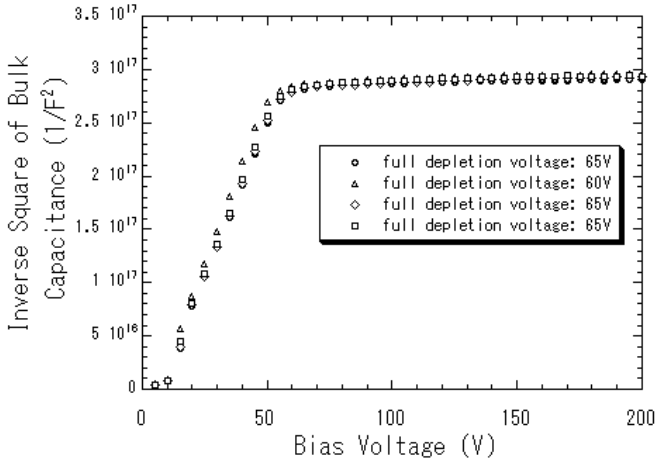

Fig. 1. The bias voltage dependence of the sensor bulk capacitance. The inverse square of the capacitance is plotted in order to clearly indicate the full depletion voltage. The different symbols refer to different sensors. The full depletion voltage of plotted four sensors is 65 V except one sensor (60 V).

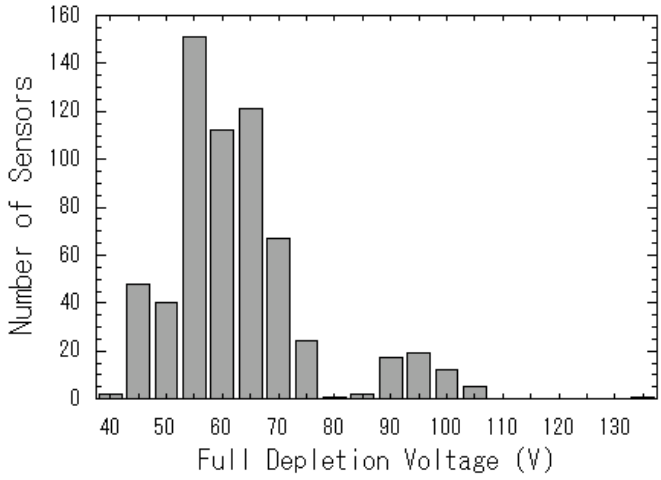

Fig. 2. The distribution of the full depletion voltage for 622 sensors. The apparent two-lobe structure in the distribution is discussed in the text.

B. Leakage Current Density

The leakage current is a strong function of the temperature with an increase by a factor two with an increase in temperature of 7.5 ^{o}C [10]. The temperature was kept constant at 25 ^{o}C during the measurements. The bias voltage dependence of the leakage current has been measured for all 622 sensors at HPK, and Fig. 3 shows the results of the measurement for the same sensors plotted in Fig. 1. The distribution of the leakage current density at 150 V bias voltage is shown in Fig. 4. The value of 150 V was chosen for the bias voltage because all sensors are fully depleted at this voltage. We anticipate that the operating voltage of the GLAST sensors is close or below 120 V. Here the leakage current density is calculated using the outside dimensions of the sensors. The average leakage current density is 2.2 ± 0.8 nA/cm^2. This value is very low and is characteristic of a very mature fabrication process and comparable to values found in photodiodes with low leakage current. We are taking advantage of such a low leakage current by testing only the total sensor current, eliminating the time consuming testing of the individual strip currents. A sensor with one or two noisy strips will show up as having excessive total current and will be marked as out of specification.

The expected I-V curve for a silicon diode has the current rising like the square root of the bias voltage up to depletion and then staying constant. The reason for the distorted I-V curves of Fig. 3 is that the voltage ramp is too fast (10 V/s). Using a much slower ramp of 1 V/min, the I-V curve takes on the expected form, as shown in Fig. 5. Yet in Fig. 5, the leakage current becomes constant around 100 V, which is larger than the full depletion voltage of this sensor of 60 V. If we employ an even slower voltage ramp, the voltage at which the current becomes constant decreases further, but the value of the current density plateau stays the same. This leakage current density at 150 V taken with a slow ramp is larger than the value of the fast ramp. By comparing the leakage current value for fast and slow ramping at a bias voltage of 150 V for 10 sensors (Fig. 6), we can determine an approximate correction factor for the fast ramp of (1.54 ± 0.14). With this correction, the true average leakage current density for 622 sensors becomes 3.4 ± 1.2 nA/cm^2. We show the need to define well the test procedures employed in the leakage current measurements, in order to be able to compare different measurements. It is clear that in production testing of large lots, one has to compromise between the time taken by the measurement and the size of the correction needed. It should be noted that in the measurements with slow ramp, all 10 sensors hold bias voltage up to 500 V without significant increase of leakage current.

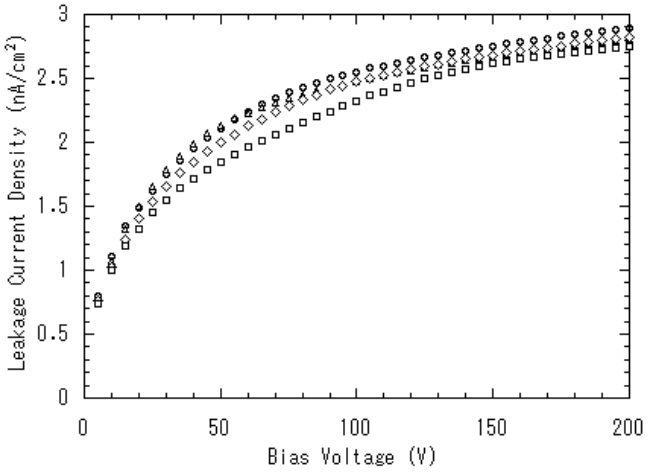

Fig. 3. The bias voltage dependence of the leakage current density at 25 °C. The sensors plotted are the ones plotted in Fig. 1.

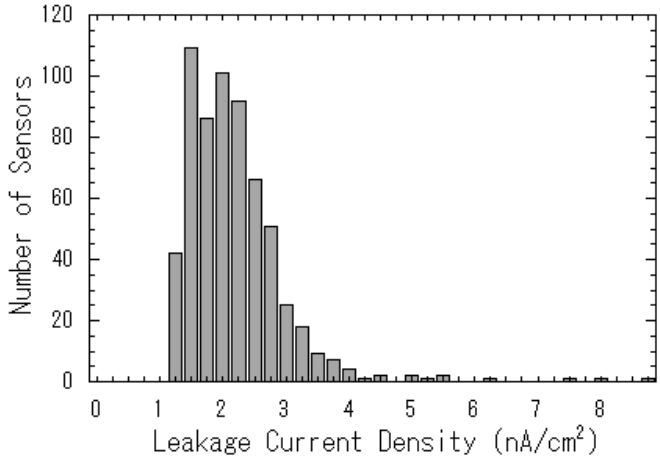

Fig. 4. The distribution of the leakage current density at 150 V bias voltage at 25°C.

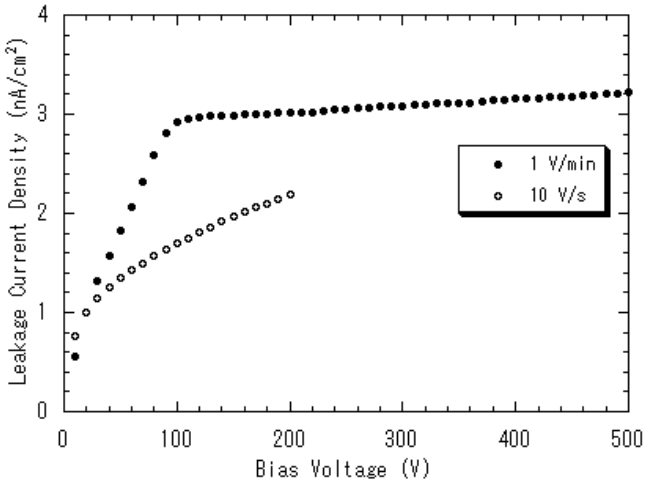

Fig. 5. The bias voltage dependence of the leakage current density at 25 °C. Open circles show the measurements with fast voltage ramp (10 V/s), solid circles show the measurements with slow ramp (1 V/min).

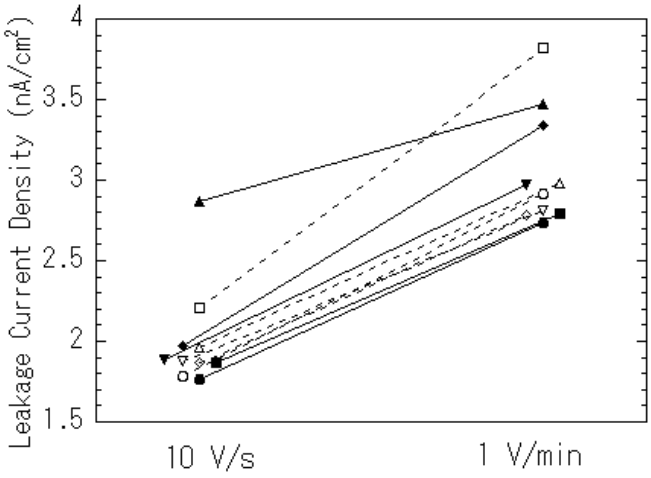

Fig. 6. The leakage current density of 10 sensors at 150 V determined with fast (10 V/s) and slow (1 V/min) voltage ramp.

C. *Faulty Strip Rate*

In total, there are 238,848 strips on 622 sensors. All strips are inspected for the failures listed in Table I. The total number of faulty strips is only 19, giving a faulty strip rate of less than 0.01 %. The results is a factor 20 lower than the specification and is extremely small compared with the sensors used in other experiments [11]. Among 622 sensors, only 14 sensors have faulty strips and about 98 % of the sensors have no faulty strips at all.

Table I
The number of faulty strips out of 238,848 strips

Shorted capacitor (aluminum strip - p^+ implant)	11
Open bias resistor	5
Open AC pad - aluminum strip	0
Bad isolation (AC pad - neighboring aluminum strip)	0
Bad isolation (DC pad - bias ring)	0
Bad isolation (DC pad - neighboring p^+ strip)	3
Total number of faulty strips	19

III. Radiation Damage

As part of the GLAST sensor quality assurance program, we are measuring the characteristics of the sensors after ^{60}Co gamma-ray irradiation, even though the on-orbit total dose is expected to be small. This will allow us to monitor the fabrication quality that effects radiation tolerance, e.g. the defect density around interface between SiO_2 layer and silicon bulk. The gamma-ray irradiation was performed in the ^{60}Co Irradiator of the Radiation Research Facility, the Faculty of Engineering, Hiroshima University. The dose rate during the irradiation was 3.8 rd(Si)/s. The dose rate was estimated from the leakage current of the sensor during the irradiation.

In order to save the "full size sensors" for the flight model (FM), "test sensors" are used for this irradiation. The test sensor and full size sensor are arranged on the same wafer and have the same layout except for the number of strips. Fabrication problem with the full size sensor will show up in

the testing of the test sensor, which will happen early enough for corrective action. The picture of the 6-inch wafer is shown in Fig. 7, with the dicing lines indicated. The test sensor has a sensitive area of 87.6 mm × 1.8 mm and eight strips.

We sampled one test sensor from every production lot of about 30 full size sensors. The test sensors were irradiated up to a total dose of 10 krd(Si). The test sensors were biased during irradiation at 150 V. After the irradiation, the test sensors were kept under 150 V bias at 20 °C until they were electrically characterized (leakage current, interstrip capacitance and interstrip isolation) one week after irradiation. So far, 10 test sensors have been irradiated.

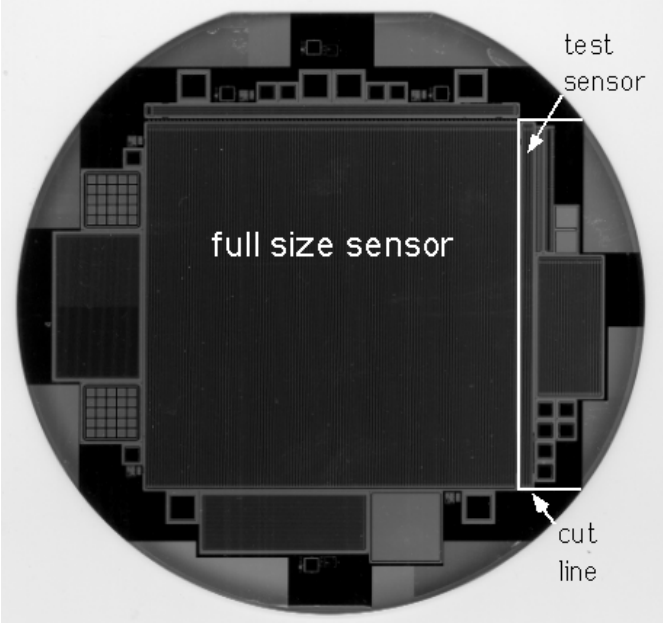

Fig. 7. The 6-inch wafer for the GLAST sensor. The big square sensor at the center is the "full size sensor" for GLAST FM. There are many test structures surrounding it. The "test sensor" is the thin structure to the right of the full size sensor.

A. Leakage Current Density

The leakage current is an important parameter of the amount of radiation damage, because it increases the shot noise in the readout [12]. Fig. 8 shows the leakage current density at 150 V bias voltage before and after irradiation. The average leakage current density before irradiation is 4.7 ± 0.8 nA/cm^2 at 25 °C. Here we calculated the leakage current density using the area inside the bias ring. The leakage current density of the test sensor exceeds the one of the full size sensors because of the effect of the cut edge. The average leakage current density a week after the irradiation was about 64 ± 13 nA/cm^2. The pre-rad and post-rad leakage currents exhibit good uniformity. The increase of leakage current after the irradiation is mainly due to surface carrier generation.

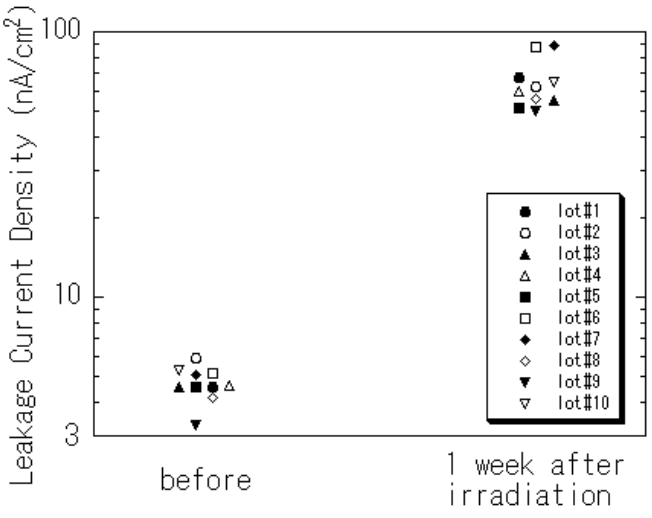

Fig. 8. The test structure leakage current density at 25 °C before and 1 week after the 10 krd ^{60}Co gamma-ray irradiation for devices biased at 150 V.

B. Interstrip Capacitance

We monitor the effect of radiation on the interstrip capacitance because a large radiation effect could indicate a problem with the surface treatment. The possible microscopic origin of the change is the radiation-induced interface traps between SiO_2 layer and silicon bulk. The amount of these traps is related to the quality of the interface [13]. In addition, the interstrip capacitance increase causes an increase of the strip load capacitance at the read-out electronics input and consequently of the noise at the read-out electronics output [14]. Fig. 9 gives a sketch of the interstrip capacitance measuring set-up. Here only the capacitance between one AC pad and its neighbors was measured at 1 MHz and evaluated with the Cp-Rp method [15]. This measures only part of the total capacitance. The total capacitance is $C_{tot} = C_{bulk} + 2C_n + C_s$ where C_{bulk} is the strip bulk capacitance, C_n is the capacitance between adjacent next neighbor Al strips and C_s is the capacitance between all other neighbor Al strips. It has been shown that measuring only C_n is sufficient to evaluate differences between the pre-rad and post-rad performance [15]. We measured the C-f curve and found it flat above a few hundred Hz. In total, there are 8 strips in the test sensors and we have measured all 6 possible combinations of $2C_n$ before and one week after the irradiation. The results are shown in Fig. 10, where the average values of the six measurements for each test sensors are shown. The average value of the six measurements for each test sensor before and after irradiation are 6.98 ± 0.15 pF and 6.73 ± 0.27 pF respectively. There was no significant difference between before and after the irradiation but the data spread increased somewhat after irradiation.

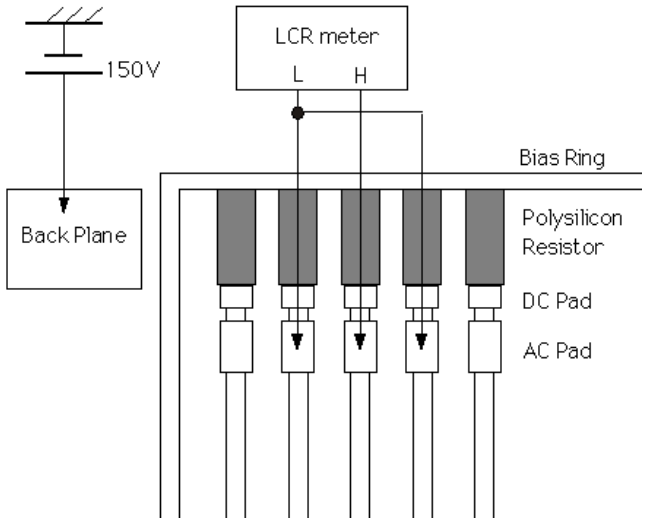

Fig. 9. The set-up for the measurement of the interstrip capacitance. The interstrip capacitance was measured at 1 MHz.

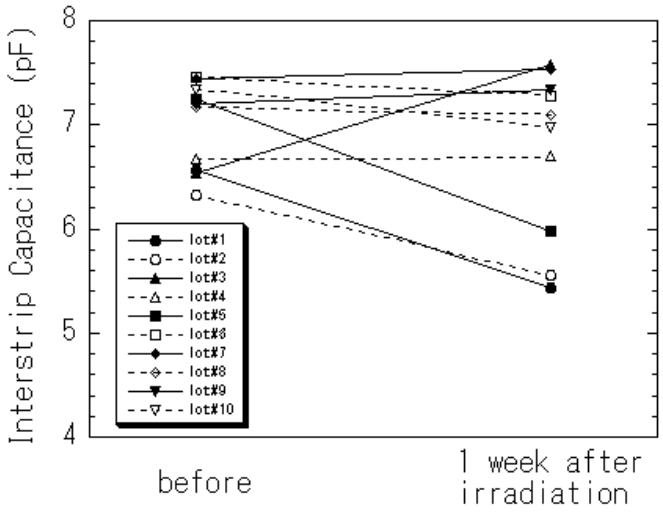

Fig. 10. The interstrip capacitance before and 1 week after the 10 krd ^{60}Co gamma-ray irradiation.

C. Interstrip Isolation

The interstrip isolation was checked in a very cursory manner, with the goal to find very large changes during irradiation like complete loss of isolation or open resistors, which is evidenced in the set-up used as shown in Fig. 11. The strips are connected to the bias ring, so the measured current is the one through the polysilicon resistor (40 MΩ) if there is no problem with the interstrip isolation. At a voltage of 1 V, the expected current (I_n) is about 25 nA. If the current is larger than 1.3 × I_n, we considered such a strip to be a faulty strip. If this kind of strip is isolated, we categorize it as "Bad isolation between DC pad and bias ring". If its neighbor has almost the same current, we categorize it as "bad isolation between DC pad and neighboring p^+ strip", i.e. bad interstrip isolation (see Table I). We can detect the bad isolation between strips with this experimental set-up if the interstrip resistance is less than 130 MΩ. The value of the interstrip resistance is usually larger than several GΩ. The results are shown in Table II. The lot number indicates the order of production. In the Table II, the number of strips whose interstrip isolation is bad are listed.

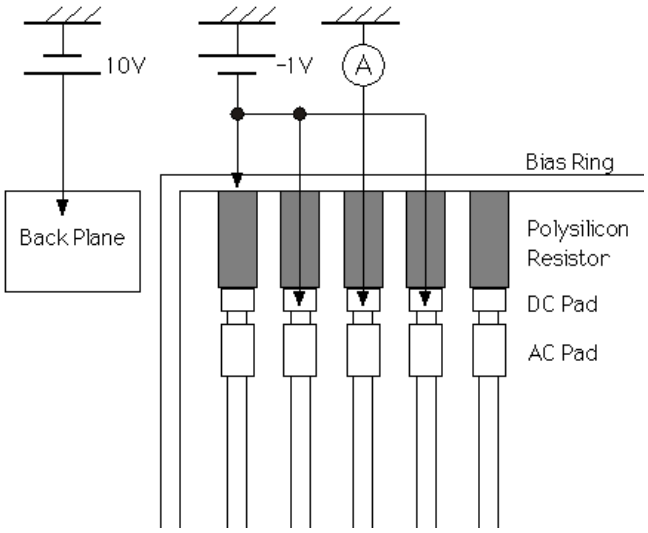

Fig. 11. The set-up for the check of interstrip isolation

Table II
The number of strips with bad interstrip isolation

Lot No.	Full size sensor	Test sensor	
	non irradiated	before iradiation	after irradiation
1	0/12672	0/8	0/8
2	0/14592	0/8	0/8
3	0/10368	0/8	0/8
4	0/11520	0/8	0/8
5	0/11904	0/8	0/8
6	0/13824	0/8	**2/8**
7	**3/10752**	**2/8**	**2/8**
8	0/9984	0/8	**2/8**
9	0/10752	0/8	0/8
10	0/13440	0/8	0/8

The notation n/m means n bad strips of m tested.

Good performance is evident: only three strips are bad out of 120k strips. Those bad strips belong to the same lot in which bad isolation was found on the test sensors, before and after irradiation. We are following up on the additional occurrence of bad isolation seen in two lots after irradiation.

IV. Conclusion

We have investigated 622 sensors for the GLAST LAT Flight Model. The full depletion voltage is found to be 63 ± 13 V, extending up to 135 V. This value is relatively low for 410 μm-thick sensors due to the use of high resistivity wafers. The leakage current density is 3.4 ± 1.2 nA/cm^2 at 25 ^{o}C. This value is comparable to a low-leakage-current photodiode. The number of faulty strips is 19 out of 240000, i.e. the rate of

faulty strips is less than 0.01 % and they affect only 2 % of tested 622 full size sensors.

We are also monitoring the radiation tolerance on test structures using ^{60}Co gamma-rays. After 10 krd, the leakage current density increased from 4.7 nA/cm^2 to 64 nA/cm^2, which is as expected. The interstrip capacitance did not change with irradiation. The interstrip isolation shows agreement between full size sensor and test sensor, and we are following up on a few cases of loss of isolation.

V. Acknowledgment

We would like to express special thanks to Professor N. Ohta for his kind help to perform the irradiation.

VI. References

[1] P. Michelson (PI), "GLAST LAT," Response to AO 99-OSS-03, Stanford Univ., 1999.

[2] E.D. Bloom ed., "Proposal for GLAST," SLAC-R-522, 1998.

[3] E. Atwood, W. Atwood, B. Bhatnager, E. Bloom, J. Broeder, V. Chen et al. "The silicon tracker of the beam test engineering model of the GLAST large-area telescope," *Nucl. Instr. Meth.* vol. A 457, pp. 126-136, 2001.

[4] D. Tournear, "The silicon tracker for the GLAST large area space telescope," *Nucl. Instr. Meth.* vol. A 473, pp. 61-66, 2001.

[5] R. C. Hartman, D. L. Bertsch, S. D. Bloom, A. W. Chen, P. Deines-Jones, J. A. Esposito, "THE THIRD CATALOG OF HIGH-ENERGY GAMMA-RAY SOURCES," *Astrophys. J. Suppl*. Vol. 123, pp. 79-202, 1999.

[6] Hartmut F.-W. Sadrozinski, "GLAST, a Gamma-Ray Large Area Space Telescope," *Nucl. Instr. Meth*. vol. A 466, pp. 292-299, 2001.

[7] W.B. Atwood J.A. Hernando, M. Hirayama, R.P. Johnson, W. Kroger, H.F.-W. Sadrozinski, "The silicon tracker/converter for the gamma-ray large area space telescope," *Nucl. Instr. Meth*. vol. A 435, pp. 224-232, 1999.

[8] GLAST Science Instrument-Space Craft Interface Requirements Document GLAST SI-SC IRD , GLAST00038, GSFC, Feb 2001.

[9] S. Yoshida, Y. Yamanaka, T. Ohsugi, H. Masuda, T.Mizuno, Y. Fukazawa et al. "Heavy ion irradiation on silicon strip sensors for GLAST," *IEEE Trans. Nucl. Sci*., submitted for publication.

[10] T. Ohsugi, A. Taketani, M. Noda, Y. Chiba, M. Asai, T. Kondo et al. "Radiation Damage in Silicon Microstrip Detectors," *Nucl. Instr. Meth.* vol. A 265, pp. 105-111, 1988.

[11] T. Ohsugi, Y. Iwata, T. Ohmoto, T. Handa, K. Fujita, H. Kitabayashi et al. "Design optimization of radiation-hard, double-sided, double-metal, AC-coupled silicon sensors," *Nucl. Instr. Meth*. vol. A 436, pp. 272-280, 1999.

[12] P. Azzi, N. Bacchetta, G. Bolla, D. Glenzinski, C.Haber, J. Incandela et al. "Radiation damage experience at CDF with SVX'," *Nucl. Instr. Meth*. vol. A 383, pp. 155-158, 1996.

[13] T. P. Ma and Paul V. Dressendorfer, "IONIZING RADIATION EFFECTS IN MOS DEVICES AND CITCUITS," John Wiley and Sons, New York, pp. 193-256, 1989.

[14] E. Barberis, N. Cartiglia, C. LeVier, J. Rahn, P. Rinaldi, H.F.W. Sadrozinski et al. "Capacitances in Silicon Microstrip Detectors," *Nucl. Instr. Meth*. vol. A 342, pp. 90-95, 1994.

[15] D. Bortoletto, A.F. Garfinkel, A.D. Hardman, K.D. Hoffman, T.A. Keaffaber, N.M. Shaw, G.R. Stanley, "Capacitance measurements of double-metal double-sided silicon microstrip detectors," *Nucl. Instr. Meth.* vol. A 383, pp. 104-109, 1996.